ISSN 1674-1056
http://cpb.iphy.ac.cn
http://iopscience.iop.org/cpb
中国物理 B
Chinese Physics
中国物理
Chinese Physics B

Influence of intra-cavity loss on transmission characteristics of fiber Bragg grating Fabry-Perot cavity

Di Wang(王迪), Meng Ding(丁孟), Hao-Yang Pi(皮浩洋), Xuan Li(李璇), Fei Yang(杨飞), Qing Ye(叶青), Hai-Wen Cai(蔡海文), Fang Wei(魏芳)
Citation: Chin. Phys. B . 2018, 27(2): 024207. **doi:** 10.1088/1674-1056/27/2/024207

Journal homepage: http://cpb.iphy.ac.cn; http://iopscience.iop.org/cpb

What follows is a list of articles you may be interested in

Optical properties of a three-dimensional chiral metamaterial

Juan-Juan Guo(郭娟娟), Mao-Sheng Wang(汪茂胜), Wan-Xia Huang(黄万霞)
Chin. Phys. B . 2017, 26(12): 124211. **doi:** 10.1088/1674-1056/26/12/124211

2-μm mode-locked nanosecond fiber laser based on MoS_2 saturable absorber

Xiao-Fa Wang(王小发), Xiao-Ling Peng(彭晓玲), Qiu-Xia Jiang(姜秋霞), Xiao-Hui Gu(顾小辉), Jun-Hong Zhang(张俊红), Xue-Feng Mao(毛雪峰), Su-Zhen Yuan(袁素贞)
Chin. Phys. B . 2017, 26(11): 114205. **doi:** 10.1088/1674-1056/26/11/114205

Code synchronization based on lumped time-delay compensation scheme with a linearly chirped fiber Bragg grating in all-optical analog-to-digital conversion

Wang Tao, Kang Zhe, Yuan Jin-Hui, Tian Ye, Yan Bin-Bin, Sang Xin-Zhu, Yu Chong-Xiu
Chin. Phys. B . 2014, 23(10): 104212. **doi:** 10.1088/1674-1056/23/10/104212

Irradiation effect on strain sensitivity coefficient of strain sensing fiber Bragg gratings

Jin Jing, Lin Song, Song Ning-Fang
Chin. Phys. B . 2014, 23(1): 014206. **doi:** 10.1088/1674-1056/23/1/014206

Experimental investigation of pre-irradiation effect on radiation sensitivity of temperature sensing fiber Bragg gratings

Jin Jing, Lin Song, Song Ning-Fang
Chin. Phys. B . 2012, 21(6): 064221. **doi:** 10.1088/1674-1056/21/6/064221

Influence of intra-cavity loss on transmission characteristics of fiber Bragg grating Fabry–Perot cavity*

Di Wang(王迪)[1,2], Meng Ding(丁孟)[1], Hao-Yang Pi(皮浩洋)[1], Xuan Li(李璇)[1], Fei Yang(杨飞)[1,†], Qing Ye(叶青)[1], Hai-Wen Cai(蔡海文)[1,‡], and Fang Wei(魏芳)[1]

[1] *Shanghai Key Laboratory of All Solid-State Laser and Applied Techniques, Shanghai Institute of Optics and Fine Mechanics, Chinese Academy of Sciences, Shanghai* 201800, *China*

[2] *University of Chinese Academy of Sciences, Beijing* 100049, *China*

(Received 22 August 2017; revised manuscript received 17 October 2017; published online 5 January 2018)

A theoretical model of the fiber Bragg grating Fabry–Perot (FBG-FP) transmission spectrum considering loss of FBG and intra-cavity fiber is presented. Several types of FBG-FPs are inscribed experimentally, and their spectra are measured. The results confirm that weak intra-cavity loss is enhanced at the resonance transmission peak, that is, loss of transmission peaks is observably larger than other wavelengths. For FBG-FPs with multi resonance peaks, when the resonance peak wavelength is closer to the Bragg wavelength, the more significant loss effect of resonance transmission peak is exhibited. The measured spectra are fitted with the presented theoretical model. The fitted coefficient of determinations are near 1, which proves the validity of the theoretical model. This study can be applied to measure FBG loss more accurately, without a reference light. It can play an important role in FBG and FBG-FP writing process optimization and application parameter optimization.

Keywords: fiber Bragg grating, Fabry–Perot cavity, intra-cavity loss, transmission characteristics

PACS: 42.81.–i, 42.81.Wg, 42.81.Dp **DOI:** 10.1088/1674-1056/27/2/024207

1. Introduction

Fiber Bragg grating Fabry–Perot cavities (FBG-FPs) are desirable for narrow-band filters and higher accuracy wavelength measurement, due to the fact that the linewidth of their ultra-narrow resonance peaks in the stopband of the fiber Bragg grating (FBGs) could easily be reduced to several MHz. Hence FBG-FP is one of the most important fiber components for lasers and suppressing noise,[1–5] tunable filters,[6–8] wavelength division multiplexing,[9] and fiber sensing.[10–12] Wei *et al.* designed an external cavity diode laser that realized a noise suppression of over 70 dB with the Fourier frequencies between 5 Hz and 1 kHz by an optical feedback ring based on FBG-FP cavity.[1] A short-linear-cavity (SLC) single-frequency fiber laser based on the slow-light effect of FBG-FP filter exhibited a several-hundred-Hz linewidth.[4] A minimum static strain resolution of $0.68n\varepsilon$ was achieved by a static-strain sensor based on FBG-FP interferometers.[12]

However, it was found that FBG-FPs transmission spectra show some loss characteristics in some practical applications. For example, the intrinsic fiber loss and the additional loss induced by ultraviolet light (UV) seriously limit the improvement of output power and linewidth of the distributed feedback (DFB) fiber laser.[13] The resonance transmission peaks of FBG-FP with high Q-factor are demanded for noise suppression demonstrated in Ref. [1]. However, it is difficult to achieve a higher Q-factor because of intra-cavity loss, which limits the performance of this configure for suppressing noise. Although the fact that the loss of FBG-FP is a significant limiting factor for its further development is well known, there are few reports with in-depth analyses on the loss characteristics in FBG-FP.

In this work, the loss characteristics of FBG-FPs are analyzed in detail. A theoretical model of the FBG-FP transmission spectrum considering FBG and intra-cavity fiber loss is established. Several types of FBG-FPs are inscribed experimentally, and fitting the measured spectrum with the theoretical model, the results show that the theoretical model is in good agreement with the experimental results. It is further demonstrated that the weak loss in FBG-FP results in ann observable reduction of resonance transmission peaks transmissivity, which is called the loss enhancement effect of resonance transmission peak in this paper. The theoretical model can be used to accurately estimate FBG loss and the loss of intra-cavity pure fiber region caused by the UV exposure. Hence it provides a new idea for the measurement of UV-induced loss.

2. Theory

The typical structure of FBG-FP consisting of two uniform single-mode FBGs with a certain distance is shown

*Project supported by the National Natural Science Foundation of China (Grant Nos. 61405212, 61377062, 61405218, and 61775225) and Scientific Innovation Fund of Chinese Academy of Sciences (Grant No. CXJJ-17S010).

†Corresponding author. E-mail: fyang@siom.ac.cn

‡Corresponding author. E-mail: hwcai@siom.ac.cn

© 2018 Chinese Physical Society and IOP Publishing Ltd

in Fig. 1. According to the FBG formation mechanism,[14] hydrogen-loading and UV exposure will induce loss to the FBG during the FBG-FP inscription process. In hydrogen-loaded fiber, H_2 molecules react at normal Si–O–Ge sites, and form Ge–OH, Si–OH, Ge–H, Si–H, and oxygen deficient Ge defects, resulting in loss increase in fiber.[15,16] FBG inscription could introduce additional extrinsic defects, such as mechanical damage, contamination, inhomogeneous index profile in the fiber core cross section,[17] and so on. These defects will cause absorption, scattering, and radiation-mode coupling in FBG.[18] In addition, post-exposing the intra-cavity pure fiber region in FBG-FP is a common method to make the transmission peak wavelength consistent with the design wavelength,[19] which would generate additional loss in the intra-cavity pure fiber region. Due to the existence of the FP effect, the weak loss will be amplified and more serious loss will be introduced at transmission peaks. In general, the main source of intra-cavity loss of FBG-FPs contains two aspects, one is the loss of FBG, and another is the loss of the intra-cavity pure fiber region.

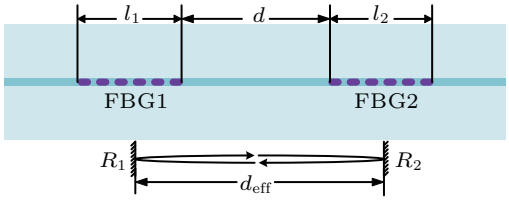


Fig. 1. (color online) Schematic diagram of FBG-FP.

The coupled mode theory is a commonly used tool for treating interactions between confined modes with refractive index perturbation, and the coupled mode equations of FBG in single fibers can be expressed as[20]

$$\frac{\mathrm{d}}{\mathrm{d}z}A = \frac{1}{2}\kappa_{11}\left(A + B\mathrm{e}^{\mathrm{j}2\beta z}\right), \tag{1a}$$

$$\frac{\mathrm{d}}{\mathrm{d}z}B = -\frac{1}{2}\kappa_{11}\left(B + A\mathrm{e}^{-\mathrm{j}2\beta z}\right), \tag{1b}$$

where $A$and B are slowly varying amplitudes for LP_{01} mode fields traveling in the $+z$ and $-z$ directions, respectively. $\kappa_{11} = -\mathrm{j}k_0(n^2 - n_0^2)/n_0$, here k_0 is the propagation constant of light in a vacuum, n_0 is the refraction index in fiber, and n is the refractive index distribution in the FBG, expressed by

$$n(z) = n_0 + \Delta\bar{n} + \Delta n\cos(k_{\mathrm{B}}z), \tag{2}$$

where $\Delta\bar{n}$ is the average refractive index increase, Δn is the amplitude of refractive index modulation, $k_{\mathrm{B}} = 2\pi/\Lambda$. Due to the existence of uniform loss, assuming that the loss coefficient is α_{f}, the complex refractive index is given by

$$\tilde{n}(z) = n(z) - \mathrm{j}\alpha_{\mathrm{f}}/k_0. \tag{3}$$

Including Eq. (3) in Eq. (1), and using the slowly varying envelope approximation, we can obtain the following pair of coupled mode equations:

$$\frac{\mathrm{d}}{\mathrm{d}z}A = -\alpha_{\mathrm{f}}A - \mathrm{j}\kappa B\mathrm{e}^{\mathrm{j}2\delta z}, \tag{4a}$$

$$\frac{\mathrm{d}}{\mathrm{d}z}B = \alpha_{\mathrm{f}}B + \mathrm{j}\kappa A\,\mathrm{e}^{-\mathrm{j}2\delta z} \tag{4b}$$

with detuning $\delta = \beta - \beta_{\mathrm{B}} = \beta - k_{\mathrm{B}}/2$, the coupling coefficient is $\kappa = \frac{1}{2}k_0\Delta n$. A and B are the slow varying functions of z, which can be divided into two parts, one is the mode coupling resulted from the refractive index periodic perturbation, and another is the amplitude attenuation caused by loss. So A and B can be written as the form: $A(z) = A_0(z)\,\mathrm{e}^{-\alpha_{\mathrm{f}}z}$, $B(z) = B_0(z)\,\mathrm{e}^{\alpha_{\mathrm{f}}z}$ and substituted into Eq. (4), the coupled mode equations can be rewritten as

$$\frac{\mathrm{d}}{\mathrm{d}z}A_0 = -\mathrm{j}\kappa B_0\mathrm{e}^{\mathrm{j}2\tilde{\delta}z}, \tag{5a}$$

$$\frac{\mathrm{d}}{\mathrm{d}z}B_0 = \mathrm{j}\kappa A_0\mathrm{e}^{-\mathrm{j}2\tilde{\delta}z}, \tag{5b}$$

where $\tilde{\delta} = \delta - \mathrm{j}\alpha_{\mathrm{f}}$. Then the reflection and transmission coefficient are solved as

$$r_{\mathrm{FBG}} = \frac{-\mathrm{j}\kappa\sinh(\tilde{\sigma}l)}{\tilde{\sigma}\cosh(\tilde{\sigma}l) + \mathrm{j}\tilde{\delta}\sinh(\tilde{\sigma}l)}, \tag{6a}$$

$$t_{\mathrm{FBG}} = \frac{\tilde{\sigma}\mathrm{e}^{-\mathrm{j}\beta_b l}}{\tilde{\sigma}\cosh(\tilde{\sigma}l) + \mathrm{j}\tilde{\delta}\sinh(\tilde{\sigma}l)}, \tag{6b}$$

where $\tilde{\sigma} = \sqrt{\kappa^2 - \tilde{\delta}^2}$. This formula has the same form with the reflection and the transmission coefficient calculation formula of the FBG without considering loss,[15] except that the detuning contains an imaginary part, which is proportional to the loss coefficient.

It is assumed that an FBG-FP is composed of two FBGs with lengths l_1 and l_2, and the distance of d between these two FBGs. According to the multi-beam interference theory,[21] the transmission coefficient of the FBG-FP shown in Fig. 1 is given by

$$t = \frac{t_1 t_2\mathrm{e}^{-\alpha_{\mathrm{c}}d}\mathrm{e}^{-\mathrm{j}\beta d}}{1 - r_1 r_2\mathrm{e}^{-2\alpha_{\mathrm{c}}d}\mathrm{e}^{-\mathrm{j}2\beta d}}, \tag{7}$$

here α_{c} is the loss coefficient of the intra-cavity pure fiber region, t_i, r_i $(i = 1,2)$ is the reflection and transmission coefficient of the two FBGs and can be solved by Eq. (6). To simplify the model, here we only analyze the loss characteristic of the FBG-FP when the FBGs are exactly the same on both sides ($l_1 = l_2 = l$, $t_1 = t_2 = t_{\mathrm{FBG}}$, $r_1 = r_2 = r_{\mathrm{FBG}}$). Then the transmission coefficient of the FBG-FP can be written as

$$t = \frac{t_{\mathrm{FBG}}^2\mathrm{e}^{-\alpha_{\mathrm{c}}d}\mathrm{e}^{-\mathrm{j}\beta d}}{1 - r_{\mathrm{FBG}}^2\mathrm{e}^{-2\alpha_{\mathrm{c}}d}\mathrm{e}^{-\mathrm{j}2\beta d}}. \tag{8}$$

We can obtain the transmissivity

$$T = \frac{T_{\mathrm{FBG}}^2\,\mathrm{e}^{-2\alpha_{\mathrm{c}}d}}{\left(1 - R_{\mathrm{FBG}}^2\,\mathrm{e}^{-2\alpha_{\mathrm{c}}d}\right)^2 + 4R_{\mathrm{FBG}}\,\mathrm{e}^{-2\alpha_{\mathrm{c}}d}\sin^2\left[\beta d + \varphi(\lambda)\right]}, \tag{9}$$

where $T_{\rm FBG}$, $R_{\rm FBG}$, and $\varphi(\lambda)$ are transmissivity, reflectivity, and reflection phase shift of the FBGs, respectively.

Here we divided the transmission spectrum of the FBG-FP into two parts for discussions, that is, the wavelength range within the stop bandwidth of the FBGs and the wavelength range outside of the stop bandwidth of the FBGs. If the wavelength is out of the stop bandwidth of the FBGs, regarding $R_{\rm FBG}$ as 0, equation (9) can be simplified as $T_{\rm FP} = T_{\rm FBG}^2 {\rm e}^{-2\alpha_{\rm c} d}$. This is the transmissivity of the light one-pass flight FBG-FP. If the wavelength is within the stop bandwidth of the FBGs, $R_{\rm FBG}$ is a function of λ. When the phase factor of Eq. (5) satisfies the resonance condition, that is, $\beta d + \varphi(\lambda) = m\pi$, the transmissivity of the FBG-FP can be given by

$$T_{\rm FP} = \frac{T_{\rm FBG}^2 {\rm e}^{-2\alpha_{\rm c} d}}{\left(1 - R_{\rm FBG}^2 {\rm e}^{-2\alpha_{\rm c} d}\right)^2}. \tag{10}$$

The transmission spectrum envelope with loss of the FBG-FP can also be calculated from Eq. (10).

3. Experiment and discussion

Firstly, the FBG-FPs are inscribed by the phase mask method as shown in Fig. 2. One diaphragm with two rectangular windows with the same length is installed in front of the phase mask. There are two sections of the same length of the UV beam exposing the phase mask and the fiber for writing the two FBG reflectors of the FBG-FP. The length of rectangular windows in the diaphragm and the distance between them are determined by the length and distance of the FBG reflectors in FBG-FPs that we designed. Two groups of FBG-FP, called group A and group B, are manufactured in SMF-28e using a KrF excimer laser with the output wavelength of 248 nm, the pulse rate of 12 Hz and single pulse energy of 80 mJ. The transmission spectra of samples in group A contain a single transmission peak and in group B contain multi transmission peaks. Each group has two samples, where A(B)-2 is obtained by post-exposing the intra-cavity pure fiber region of A(B)-1. The parameters of FBG-FP inscription are described in detail in Table 1.

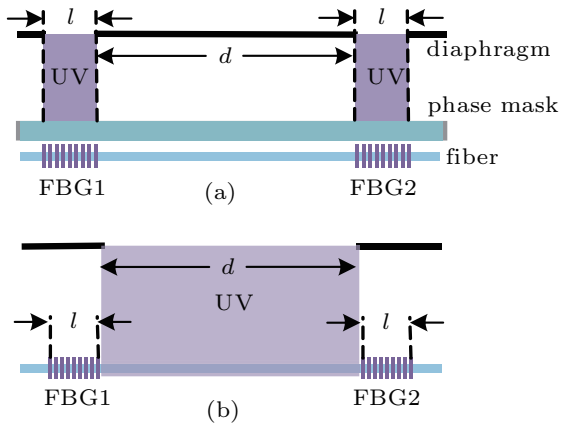


Fig. 2. (color online) Schematic diagram of FBG-FP inscription (a) A(B)-1; (b) A(B)-2.

Table 1. Parameters of FBG-FP inscription.

	l/mm	d/mm	Pulse counts of UV uniform exposure
A-1	8.5	2	0
A-2	8.5	2	4000
B-1	3	13	0
B-2	3	13	3000

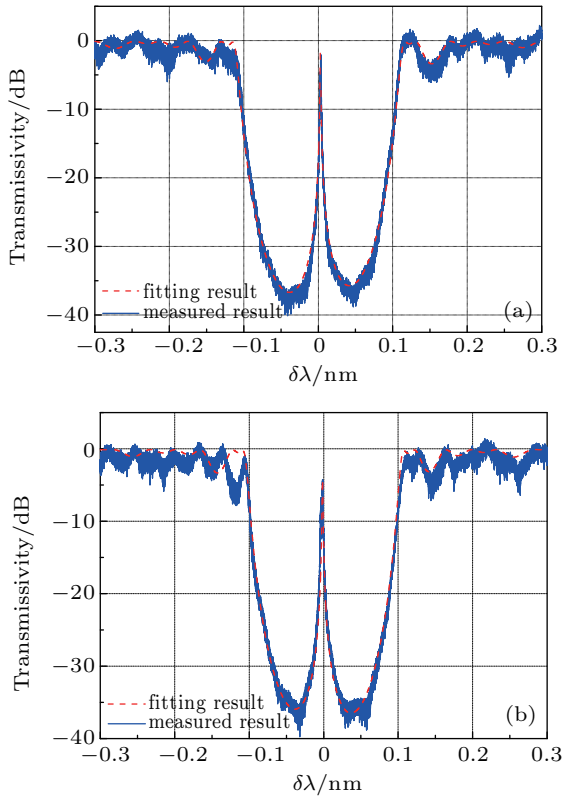


Fig. 3. (color online) Spectra of FBG-FP in group A, where blue solid curves are measured results and red dash curves are fitting results (a) A-1; (b) A-2.

The spectra of FBG-FPs are monitored using an optical spectrum analyzer (OSA) with a resolution of 0.04 pm (APEX Technologies, AP-2041B). The probe light is provided by the OSA's affiliated tunable laser with a linewidth of 500 kHz. The spectra of FBG-FPs of two groups are shown in Fig. 3 and Fig. 4, respectively, where blue solid curves are measured results and red dashed curves are results fitting with Eq. (9) in section 2. Fitting parameters of A-1 and A-2 in Fig. 3 are $\kappa = 0.33$ mm^{-1}, $\alpha_{\rm f} = 0.00055$ mm^{-1}, $\alpha_{\rm c} = 0$ mm^{-1}, and $\kappa = 0.32$ mm^{-1}, $\alpha_{\rm f} = 0.00055$ mm^{-1}, $\alpha_{\rm c} = 0.0014$ mm^{-1}, respectively. The fitted coefficient of determination R^2 are 0.9932 and 0.9859, respectively. It is seen that the theoretical model is in good agreement with the experimental results, and confirms that the theoretical model is valid for calculating the FBG-FP spectrum. In the ideal case, the transmissivity of the transmission peak should be 100%, but if there is a weak intra-cavity loss, the transmissivity of the resonance transmission peak is reduced obviously. The loss of the resonance transmission peak in samples A-1 and A-2 are 2.07 dB and 3.76 dB, respectively. These loss values are much greater

than UV- induced loss in fiber, which indicates that the resonance effect enhances the loss of the resonance transmission peak. This phenomenon is called the loss enhancement effect of the resonance transmission peak in this paper.

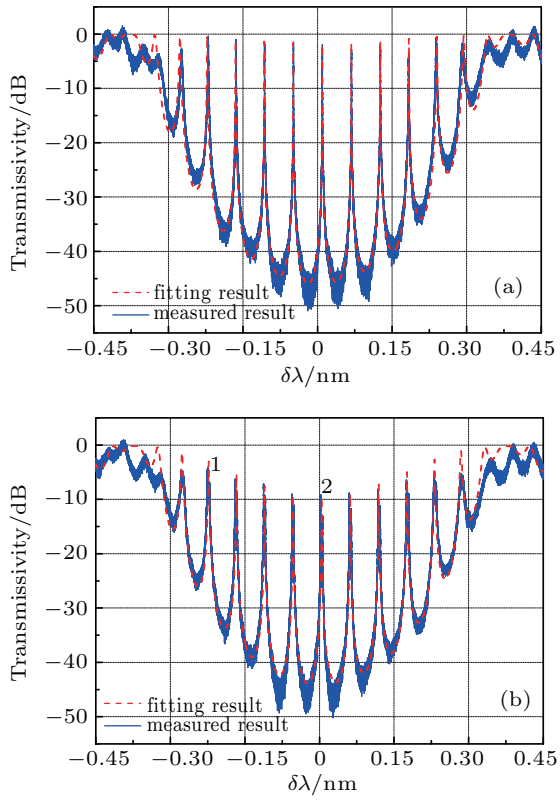


Fig. 4. (color online) Spectra of FBG-FP in group B, where blue solid curves are measured results and red dash curves are fitting results (a) B-1; (b) B-2.

Fitting parameters of B-1 and B-2 in Fig. 4 are $\kappa = 1\ \text{mm}^{-1}$, $\alpha_f = 0.0011\ \text{mm}^{-1}$, $\alpha_c = 0\ \text{mm}^{-1}$, and $\kappa = 0.96\ \text{mm}^{-1}$, $\alpha_f = 0.0011\ \text{mm}^{-1}$, $\alpha_c = 0.00085\ \text{mm}^{-1}$, respectively. The coefficient of the determination R^2 are 0.9604 and 0.9662, respectively. The results illustrate that loss values are related with the wavelength of light. For example, in Fig. 4(b), the loss of peak 1 is 4.13 dB, and the loss of peak 2 is 9.10 dB. This phenomenon is attributed to the FP resonant effect. The light components at the transmission wavelength repeatedly oscillate, resulting in experiencing longer optical paths before it transmits out. Thus it suffers much more loss than a single path. The number of round trips, or photon lifetime, is related with the reflection of FBG at the transmission peak wavelength. Hence, the higher the reflectivity is, the more significant the loss enhancement effect of the resonance transmission peak is exhibited. Figure 5 shows the FBG-FP transmission spectrum and its envelope calculated with Eq. (10), the parameters are the same as the fitted values of FBG-FP in group B. The pink dotted curve, blue solid line, and red dashed line present the reflection spectrum of single FBG, transmission spectrum of FBG-FP, and envelope of the transmission spectrum respectively. It can be seen that the transmission wavelength is closer to the Bragg wavelength, then the single FBG reflectivity is higher, and the loss is more remarkable.

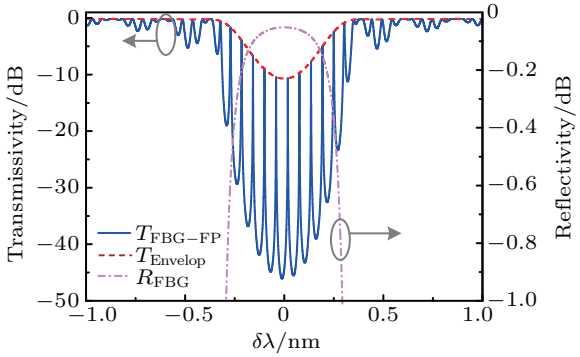


Fig. 5. (color online) Simulation of the FBG-FP using Group B's parameter with $\kappa = 1\ \text{mm}^{-1}$, $\alpha_f = 0.0011\ \text{mm}^{-1}$, $\alpha_c = 0.00085$ mm.

The post-exposure induced loss for FBG-FP is shown in Fig. 3(b) and Fig. 4(b). According to the fitting parameters, we estimate that loss of about $0.0014\ \text{mm}^{-1}$ is induced by 4000-pulse counts uniform UV-exposure, and 3000-pulse counts UV-exposure results in loss of $0.00085\ \text{mm}^{-1}$. It provides a new way to measure UV-induced loss. In the past, in order to avoid some disturbing factors, such as fiber splicing loss, measuring a spectrum as reference before FBG is written and monitoring the spectrum during FBG writing were used to estimate UV-induced loss.[22] This method is limited by the accuracy of OSA, whose accuracy generally is 0.01 dB. Besides it is useless after annealing. We demonstrated that the photothermal effect in phase shift FBG can be used to estimate the loss coefficient of FBG in previous work.[23] However, the measurement error is large by this method, due to the fact that the heat dissipation condition have a strong impact on the transmission peak drift of the phase shift FBG. So it is expected to be a new method to measure UV-induced loss by using the loss enhancement effect of the transmission peak, which can increase the accuracy by two orders of magnitude without reference light.

4. Conclusion

In this paper we analyzed the effect of the UV-induced loss on the spectral response of FBG-FPs. The theoretical study is achieved by extending the standard coupled-mode theory including the effect of periodic loss and the multi-beam interference theory including the intra-cavity fiber loss. Several FBG-FPs with a single resonance peak or multi-resonance peaks are manufactured in experiments, and the measured spectrum is fitted with the theoretical model in Section 2; the theoretical result is in good agreement with the experimental results. It is demonstrated that the weak loss in FBG-FP results in serious reduction of resonance transmission peaks transmissivity. For FBG-FP with multi-resonance peaks, the resonance peak wavelength is closer to the Bragg wavelength, the more

significant the loss effect of the resonance transmission peak is exhibited. This study can be applied to measure FBG loss more accurately, without reference light, and it can play an important role in FBG and FBG-FP writing process optimization and application parameter optimization.

References

[1] Wei F, Yang F, Zhang X, Xu D, Ding M, Zhang L, Chen D J, Cai H W, Fang Z J and Gu X J 2016 *Opt. Express* **24** 17406

[2] Cheng X P, Shum P, Tse C H; Zhou J L, Tang M, Tan W C, Wu R F and Zhang J 2008 *IEEE Photon. Technol. Lett.* **20** 976

[3] Du Y, Dong X P, Chen M X and Zhou J L 2012 *Microwave Opt. Technol. Lett.* **54** 1230

[4] Mo S P, Huang X, Xu S H, Feng Z M, Li C, Yang C S and Yang Z M 2015 *Appl. Phys. Express* **8** 082703

[5] Geng D, Yang D X, Shen G F and Zhang X M 2008 *Chin. Phys. B* **17** 1020

[6] Tao R C, Feng X H, Cao Y, Li Z H and Guan B O 2012 *IEEE Photon. Technol. Lett.* **24** 1805

[7] Li Y, Zhou B, Zhang L and He S L 2015 *Opt. Commun.* **344** 156

[8] Kim T Y, Hanawa M, Kim S J, Hann S, Kim Y H, Han W T and Park C S 2006 *Opt. Express* **14** 4250

[9] Chow J, Town G, Eggleton B, Ibsen M, Sugden K and Bennion I 1996 *IEEE Photon. Technol. Lett.* **8** 60

[10] Cranch G A, Flockhart G M H, and Kirkendall C K 2005 *J. Lightwave Technol.* **23** 3798

[11] Miridonov S V, Shlyagin M G and Tentori D 2001 *Opt. Commun.* **191** 253

[12] Liu P D, Huang W Z, Zhang W T and Li F 2017 *IEEE Photon. Technol. Lett.* **29** 814

[13] Lauridsen V C, Povlsen J H and Varming P 1999 *Electron. Lett.* **35** 300

[14] Kashyap R 2009 *Fiber Bragg Gratings*, 2nd edn. (Oxford: Academic Press) pp. 36–38

[15] Zabezhailov M O, Tomashuk A L, Nikolin I V and Golant K M 2001 *Proceedings of the Radiation and Its Effects on Components and Systems*, September 10–14, 2001, Grenoble, France, p. 192

[16] An H, Cui X, Wen P, Lin X, LIU H, Pun E Y B and Chung P S 1997 *Chin. Phys. Lett.* **14** 187

[17] Bernard P, Bessard J, Brochu G and Lemaire É 2011 *Proceedings of the Fiber Laser Applications*, February 16–17, Istanbul, Turkey, p. FThE12

[18] Johlen D, Knappe F, Renner H and Brinkmeyer E 1999 *Optical Fiber Communication Conference*, February 21–26, 1999, San Diego, USA, p. ThD1

[19] Canning J and Sceats M G 1994 *Electron. Lett.* **30** 1344

[20] Li S F, Li C R and Song C L 2013 *Fundamentals of Optical Waveguide Theory* (Beijing: Electronic Industry Press) p. 109

[21] Yariv A and Yeh P 2007 *Photonics: Optical Electronics in Modern Communications*, 6th edn. (New York: Oxford University Press) p. 239

[22] Littler I C M, Grujic T and Eggleton B J 2006 *Appl. Opt.* **45** 4679

[23] Ding M, Chen D J, Fang Z J, Wang D, Zhang X, Wei F, Yang F, Ying K and Cai H W 2016 *Opt. Express* **24** 25370